

# Ultraviolet and visible photometry of asteroid (21) Lutetia using the Hubble Space Telescope <sup>★</sup>

H. A. Weaver<sup>1</sup>, P. D. Feldman<sup>2</sup>, W. J. Merline<sup>3</sup>, M. J. Mutchler<sup>4</sup>, M. F. A'Hearn<sup>5</sup>, J.-L. Bertaux<sup>6</sup>, L. M. Feaga<sup>5</sup>, J. W. Parker<sup>3</sup>, D. C. Slater<sup>7</sup>, A. J. Steffl<sup>3</sup>, C. R. Chapman<sup>3</sup>, J. D. Drummond<sup>8</sup>, and S. A. Stern<sup>9</sup>

<sup>1</sup> Johns Hopkins University Applied Physics Laboratory, Space Department, 11100 Johns Hopkins Road, Laurel, MD 20723-6099 USA e-mail: hal.weaver@jhuapl.edu

<sup>2</sup> Johns Hopkins University, Department of Physics and Astronomy, 3100 N. Charles Street, Baltimore, MD 21218 USA

<sup>3</sup> Southwest Research Institute, Department of Space Studies, Suite 300, 1050 Walnut Street, Boulder CO 80302-5150 USA

<sup>4</sup> Space Telescope Science Institute, 3900 San Martin Drive, Baltimore, MD 21218 USA

<sup>5</sup> Department of Astronomy, University of Maryland, College Park MD 20742-2421 USA

<sup>6</sup> Service d'Aéronomie, Réduit de Verrières – BP3, Routes des Gatines, 91371 Verrières le Buisson Cédex, France

<sup>7</sup> Southwest Research Institute, P. O. Drawer 28510, San Antonio TX 78228-0510 USA

<sup>8</sup> Starfire Optical Range, Air Force Research Laboratory, Kirtland Air Force Base, Albuquerque, NM 87117 USA

<sup>9</sup> Southwest Research Institute, Space Division, 1050 Walnut Street, Boulder, CO 80302-5150 USA

Received 23 December 2009 / Accepted 27 June 2010

## ABSTRACT

**Context.** The asteroid (21) Lutetia is the target of a planned close encounter by the *Rosetta* spacecraft in July 2010. To prepare for that flyby, Lutetia has been extensively observed by a variety of astronomical facilities.

**Aims.** We used the *Hubble Space Telescope* (*HST*) to determine the albedo of Lutetia over a wide wavelength range, extending from  $\sim 1500$  Å to  $\sim 7000$  Å.

**Methods.** Using data from a variety of *HST* filters and a ground-based visible light spectrum, we employed synthetic photometry techniques to derive absolute fluxes for Lutetia. New results from ground-based measurements of Lutetia's size and shape were used to convert the absolute fluxes into albedos.

**Results.** We present our best model for the spectral energy distribution of Lutetia over the wavelength range 1200–8000 Å. There appears to be a steep drop in the albedo (by a factor of  $\sim 2$ ) for wavelengths shorter than  $\sim 3000$  Å. Nevertheless, the far ultraviolet albedo of Lutetia ( $\sim 10\%$ ) is considerably larger than that of typical C-chondrite material ( $\sim 4\%$ ). The geometric albedo at 5500 Å is  $16.5 \pm 1\%$ .

**Conclusions.** Lutetia's reflectivity is not consistent with a metal-dominated surface at infrared or radar wavelengths, and its albedo at all wavelengths (UV-visible-IR-radar) is larger than observed for typical primitive, chondritic material. We derive a relatively high FUV albedo of  $\sim 10\%$ , a result that will be tested by observations with the *Alice* spectrograph during the *Rosetta* flyby of Lutetia in July 2010.

**Key words.** Minor planets, asteroids

## 1. Introduction

The *Rosetta* spacecraft was launched on 2 March 2004 and is heading toward an historic encounter with comet 67P/Cheryumov-Gerasimenko (67P/C-G) in 2014. Along the way, *Rosetta* has flyby encounters with two asteroids: the spacecraft passed at a distance of 803 km from (2867) Steins on 5 September 2008, and an encounter with (21) Lutetia is currently being planned for a flyby distance of  $\sim 3000$  km on 10 July 2010. Barucci et al. (2007) provide an excellent summary of the pre-2006 data accumulated for both of these asteroids. The first results from the *Rosetta* flyby of Steins have recently been published in *Science* (Keller et al. 2010) and in a special volume of *Planetary and Space Science* (2010).

To assist with the planning of the Lutetia flyby, we made observations of this asteroid with the *Hubble Space Telescope*

(*HST*) in late-November and early-December 2008, near the time of opposition when both the solar phase angle and the geocentric distance were minimized. The objectives of the program were:

1. To measure the far ultraviolet ( $\lambda \approx 1500$  Å) albedo of Lutetia to enable better planning of the flyby observations by the *Alice* ultraviolet (UV) spectral imager (Stern et al. 2007).
2. To measure the near UV ( $\lambda \approx 2000 - 3000$  Å) and visible ( $\lambda \approx 4000 - 7000$  Å) albedo, thereby providing the spectral energy distribution across a wide wavelength range and possibly yielding improved insights into the nature of the surface composition and taxonomic class of Lutetia.
3. To search for dust debris and companions near Lutetia that might pose a hazard to the *Rosetta* spacecraft, using deep, visible-band observations.
4. To use spatially resolved *HST* images of Lutetia to constrain its size and shape.

In this paper, we focus on the first two objectives, providing the best available pre-flyby estimates of the UV-to-visible spec-

<sup>★</sup> Support for this work was provided by NASA through a grant from the Space Telescope Science Institute (program #11957), which is operated by the Association of Universities for Research in Astronomy, Incorporated, under NASA contract NAS5-26555.

tral energy distribution of Lutetia. The other objectives will be discussed in separate, future publications.

## 2. Observations, Data Reduction, and Results

We were granted Director’s Discretionary Time (program ID 11957) on *HST* to perform filter photometry of Lutetia in support of the *Rosetta* flyby in July 2010. We were initially allocated 5 orbits (synonymous with “visits” in this case) of observing time, which were executed successfully on 30 November 2008, when Lutetia’s heliocentric distance ( $r$ ) was 2.42 AU, the geocentric distance ( $\Delta$ ) was 1.44 AU, and the solar phase angle ( $\phi$ ) was 0°:47–0°:48. When a preliminary analysis of those data suggested the presence of a previously unknown companion to Lutetia (subsequently determined to be an optical ghost), we were allocated 2 more orbits of *HST* time, one of which executed successfully on 15 December 2008 ( $r = 2.45$  AU,  $\Delta = 1.50$  AU,  $\phi = 7^{\circ}:52$ ) and the other executed successfully one day later ( $r = 2.45$  AU,  $\Delta = 1.50$  AU,  $\phi = 7^{\circ}:98$ ). Table 1 provides a log of all the *HST* observations, detailing the rootnames for the data files, the time span of each visit, the instrument used, the filters employed, the image exposure times, and the objectives of each visit.

For our program, we employed two different instruments: the Planetary Camera (PC) mode of the Wide Field Planetary Camera 2 (WFPC2) was used for the filter photometry covering the near-ultraviolet (NUV) and visible wavelength ranges, while the Solar Blind Channel (SBC) of the Advanced Camera for Surveys (ACS) was used to measure the far-ultraviolet (FUV) flux. The WFPC2/PC has square pixels 0’046 on a side, and the ACS/SBC has (after *drizzling* to remove geometrical distortion) square pixels 0’025 on a side. In both cases, we used the standard calibrated images from the processing pipeline operated by the Space Telescope Science Institute (STScI).

Because multiple images were obtained for the WFPC2 observations, at two different positions on the detector (to mitigate the effects of cosmic rays and bad CCD pixels), we generally combined them to produce a single, composite image that was used for photometric analysis. Figure 1 shows example composite images for the F218W, F255W, F300W, and F450W filters. The ratio of the signals from the F450W and F606W images taken on Dec 15 was used to normalize the F450W photometry to the same absolute scale as the photometry taken on Nov 30. Figure 2 shows all the individual images (not composites) for the short (0.11 s) exposures taken with the F606W filter. The electronic gain for the 0.11 s images taken through F606W filter was half the value used for the other WFPC2 images because Lutetia is bright ( $V \approx 10.1$ ), and we needed the extra dynamic range provided by the lower gain setting (0.11 s is the shortest available exposure time for the WFPC2).

The ACS/SBC employs a photon-counting detector that is essentially insensitive to cosmic ray contamination, so we simply took a single, long exposure at a single location on the detector for our FUV imaging. The four images (2 for F140LP and 2 for F165LP) are displayed in figure 3. Unfortunately, a star passing near Lutetia contaminated the F165LP image taken during visit 05, rendering the photometry unusable for that observation. Although the FUV photometry was obtained  $\sim 75$  min after the photometry taken through the other filters, we did not attempt to correct the FUV photometry for any light curve variation because that effect was determined to be  $\sim 4\%$  (using the shape model from Drummond et al. 2010), whereas the statistical error in the F140LP–F165LP photometry is  $\sim 17\%$  (see below).

We used standard circular aperture photometry to determine the total signal in each *HST* filter. We then compared the observed signal to the predicted signal using a model Lutetia albedo spectrum and measured *HST* throughput curves (a technique called *synthetic photometry*). We iteratively adjusted the albedo model until the *measured* count rates from the *HST* filter photometry matched the *predicted* values from synthetic photometry to within the measurement uncertainties. In addition to the Hubble photometry, we used a ground-based spectrum taken on 28 November 2008 (Perna et al. 2010), just two days prior to the first *HST* observations, to constrain the slope of Lutetia’s albedo at visible wavelengths. All albedos discussed here refer to the *geometric albedo*, which is the albedo at a solar phase angle of 0°. We adopted a phase correction factor of 0.91 when converting fluxes from a phase angle of 0° to the observed phase angle of 0°:48 on 2008 November 30, which is consistent with the phase law deduced from visible observations (Belskaya et al. 2010).

In coordination with our *HST* effort, we acquired high-angular resolution adaptive-optics imaging at the Keck Telescope near the times of the 2008 opposition. We combined these data with data previously acquired at the Very Large Telescope (VLT) near the prior opposition, in June 2007, to provide improved estimates of the size, shape, and spin axis of Lutetia, and also to search for satellites (Carry et al. 2010; Drummond et al. 2010; Merline et al. 2010). We adopt here the hybrid shape model derived by combining the results from the direct size measurements and the inversion of various light curve data (Carry et al. 2010; Drummond et al. 2010). This model is then used to predict Lutetia’s projected area at the time of the *HST* observations. The predicted projected area varies between 9615 km<sup>2</sup> and 10081 km<sup>2</sup> over the course of the *HST* observations, and this variation of  $\sim 4.8\%$  is within the expected uncertainty in the prediction itself ( $\sim 6\%$ ). We have adopted a projected area of 10000 km<sup>2</sup>, corresponding to an effective diameter for Lutetia of 113 km, to set the absolute scale for the albedo. (Note that the *mean* 3-dimensional diameter of Lutetia is 105 km, as determined by Drummond et al. 2010. But when viewed from high latitudes, or close to pole-on, the effective diameter of the projected disk is larger, due to viewing primarily the a,b dimensions. An independent size estimate can be derived from the *HST* images because Lutetia is slightly resolved, but detailed modeling is required to derive accurate size and shape estimates, and we are deferring this work to a future paper.) We estimate that the uncertainty in the albedo derived below is  $\sim 6\%$ .

We used the solar spectrum from Colina et al. (1996) to convert from albedo to absolute fluxes. Table 2 summarizes the numerical results after the final iteration, and figure 4 displays our best estimate for Lutetia’s absolute flux at the time of the first *HST* observations on 30.726 November 2008.

Applying synthetic photometry to the *HST* data is essential for obtaining accurate results because Lutetia’s flux varies dramatically across the passbands of all the filters used, except F450W and F606W. Figure 5 shows the predicted count rates as a function of wavelength for each of the filters employed during the *HST* observations, as well as the response for the difference F140LP–F165LP. Determination of the FUV flux is especially problematic owing to “red leak” issues (i.e., when much, or even most, of the observed signal is produced by photons whose wavelengths are much longer than the wavelength of the peak in the filter transmittance), which figure 5 graphically illustrates. For the F140LP filter, only  $\sim 10\%$  of the observed signal is produced by photons having wavelengths shortward of 1895 Å. For F165LP, only  $\sim 10\%$  of the observed signal is produced by

photons having wavelengths shortward of 1975 Å. The 50% point (i.e., half the observed signal is produced by photons either shortward or longward of that wavelength) occurs at 3340 Å for F140LP and 3390 Å for F160LP. We mitigate the red leak problem by forming the difference signal (F140LP–F165LP), which significantly improves the situation, as indicated in figure 6. In that case, ~40% of the difference signal is produced by photons having wavelengths shortward of 1675 Å, and the 50% point occurs at 2400 Å. Nevertheless, the red leak remains a major issue affecting the accuracy of our FUV results.

In order to match the measured signals for the F140LP and the F165LP filters, and additionally match their *difference* signal (F140LP–F165LP), we had to increase the system throughput (QT) for each of those filters by a factor of 2.5 for wavelengths longward of 2000 Å, relative to the curves currently adopted by the STScI (i.e., the red leak is even worse than originally thought). After consultation with the relevant experts at the STScI, we concluded that the large uncertainty in the long wavelength response of the FUV filters justifies our empirical approach. While our choice for the filter throughputs is certainly not unique, and may be incorrect in detail, we are confident in our assessment that a red leak adjustment for the F140LP and F165LP filters, of approximately the magnitude adopted here, is required to produce consistent results.

Additional information on Lutetia’s UV albedo is available from *IUE* observations performed in 1982, originally analyzed by Roettger & Buratti (1994). We obtained these data from the STScI archive, and reanalyzed them using new information on the phase behavior (Belskaya et al. 2010) and size of Lutetia (Drummond et al. 2010). The *IUE* spectrum (figure 7) is noisy and was taken at a solar phase angle of 26.1, making the correction to geometric albedo rather uncertain. Adopting a phase correction factor of 3.1, which is the value observed for Lutetia at visible wavelengths, we obtain an average albedo of ~0.14 near 2670 Å. The latter is double the value adopted by Roettger & Buratti (1994) (0.074, after correction to the new effective diameter), apparently owing to their use of a different phase law. The phase law typically depends on both the absolute albedo and the wavelength. Thus, it is not surprising that our phase correction factor is significantly different than the one adopted by Roettger & Buratti (1994), especially since there is scant data available on the phase behavior of Lutetia at UV wavelengths. In order to match the *HST* photometry from the F255W filter, we adopted an albedo of ~0.10 near 2670 Å, which is approximately halfway between the two different *IUE* results.

Of greater concern is the slope of Lutetia’s albedo between 2400 Å and 3300 Å. The *HST* data suggest there is a sharp drop in Lutetia’s albedo in the wavelength range ~3000–3300 Å, while the *IUE* data indicate that the albedo is essentially constant over the wavelength range ~2400–3300 Å. Although the *IUE* observations were performed nearly 27 years before the *HST* observations, we would not expect the UV albedo of Lutetia to change either in its slope or its absolute value over that time. The aspect angles of the *HST* and *IUE* observations were significantly different (Lutetia’s sub-Earth latitude was  $-73^\circ$  during the *HST* observations and  $-51^\circ$  during the *IUE* observations), and perhaps albedo variation over Lutetia’s albedo could explain the differences in the *HST* and *IUE* results. However, the long exposure time for the *IUE* spectrum (3.2 hr) covered nearly 75% of Lutetia’s lightcurve period, suggesting that surface variegation may not play a significant role. In summary, there appears to be a discrepancy between the *IUE* and *HST* results for the slope of Lutetia’s UV albedo near 3100 Å. Nevertheless, both

the *IUE* and *HST* data indicate that the NUV albedo is significantly smaller than the visible albedo. The *HST* data further suggest that the FUV albedo is approximately 60% of the visible albedo.

### 3. Discussion

Lutetia was extensively observed in the 1970s, yielding visible and near-IR reflectance spectra (McCord & Chapman 1975), radiometric albedos and diameter estimates (Morrison 1977), and polarimetric albedos and diameter estimates (Zellner & Gradie 1976), which have been confirmed by similar observations reported during the last decade (see Belskaya et al. 2010). Based on these data, Chapman et al. (1975) assigned Psyche, Lutetia, and Kalliope to a new, distinct taxonomic group, to which Zellner & Gradie (1976) assigned the letter “M”.

The M-type was defined in terms of spectral and albedo properties by Bowell et al. (1978). Although the visual albedos for M-class objects covered a broad range (~7–23%), they were larger than the albedos for typical carbonaceous chondrites (CC) and overlapped the range reported for S-types. Recent radiometry of Lutetia, reduced using two different thermal models, confirmed that Lutetia’s visual albedo is higher than for typical CC meteorites (Mueller et al. 2006). However, some types of CCs (CO/CV) have visual albedos approaching ~16% (Clark et al. 2009), essentially identical to the value derived here for Lutetia from the *HST* observations.

Rivkin et al. (1995) recognized that there were two subclasses of M-type asteroids. The standard M types had high radar albedos and relatively neutral visible colors, properties that could be attributed to metal-dominated surfaces. But some of the M type asteroids, including Lutetia, had an absorption band near 3  $\mu\text{m}$  band, which was attributed to hydrated minerals. Rivkin et al. (2000) call this new “wet” class M(W) and assigned Lutetia to it.

Radar observations of Lutetia (Magri et al. 1999, 2007), confirmed by Shepard et al. (2008), showed that Lutetia has a moderate radar albedo: nominally ~20%, but possibly as low as 10% or as high as 31% after accounting for the error bars. Lutetia’s radar albedo is lower than for the largely metallic asteroids but is somewhat higher than for typical CCs (13%  $\pm$  5% for the average C-class object, according to Shepard et al. 2008).

Numerous researchers in the last few years (Barucci et al. 2005, 2008; Lazzarin et al. 2009; Perna et al. 2010; see summary by Belskaya et al. 2010) have argued that Lutetia shows certain spectral characteristics (e.g., in the thermal IR) that resemble several CO and CV meteorites, but not an iron meteorite. However, mineralogical interpretations of thermal IR spectra must be made cautiously because particle size, in addition to composition, can strongly affect the observed spectral features (Vernazza et al. 2010). We further note that: (a) the lack of a drop-off in Lutetia’s spectral reflectance below 0.55  $\mu\text{m}$  and its relatively high albedo make it inconsistent with CV meteorites (see Gaffey 1976, for instance), and (b) CO meteorites display a 1  $\mu\text{m}$  olivine band that is absent in Lutetia’s reflectance spectrum (see Fig. 3 of Barucci et al. 2005).

It was first suggested by Chapman & Salisbury (1973) that what we now term an M-type spectrum might be associated with enstatite chondrites (ECs). More recently, Rivkin et al. (2000) have suggested that a hydrated EC is a plausible composition for Lutetia, consistent with the recent analysis of Vernazza et al. 2009. From rotationally resolved visible and near-IR spectra of Lutetia, Nedelcu et al. (2007) claimed a better match with CC in



one hemisphere and with EC in the other, but this hemispherical spectral asymmetry has not yet been confirmed by other researchers.

Recent dynamical work (Baer et al. 2008; Fienga et al. 2009) has provided an estimate for Lutetia's mass, which combined with the new size estimates (Drummond et al. 2010; Carry et al. 2010) yield a bulk density of  $\sim 4 \text{ g cm}^{-3}$  (the formal uncertainty ranges from 2.4–5.1  $\text{g cm}^{-3}$ ; see Drummond et al. 2010). This density is too small for an object having a dominantly metal component and seems more compatible with an EC-like composition (Drummond et al. 2010).

As discussed by Roettger & Buratti (1994), the slope of Lutetia's NUV albedo is similar to that of the M- and S-type asteroids observed by *IUE*. The albedo of the C-type asteroids observed by *IUE* increases (by  $\sim 10\%$ ) between 2400 Å and 3000 Å, whereas there is little to no variation in Lutetia's albedo over this wavelength range. Both the *IUE* and *HST* data demonstrate that the absolute value of Lutetia's NUV albedo is larger than typically observed for the C-type asteroids.

According to the *HST* data, Lutetia has a rather high FUV albedo of  $\sim 10\%$  over the entire wavelength range from  $\sim 1500$  Å to  $\sim 3000$  Å. This can be compared to an FUV albedo of  $\sim 4\%$  for the Earth's Moon (Henry et al. 1995) and the E-type asteroid 2867 Steins (A'Hearn et al. 2010), the only asteroid observed at FUV wavelengths. Furthermore, neither the Moon nor Steins show an abrupt drop in albedo near 3200 Å.

We compared Lutetia's albedo to laboratory reflectivity measurements of a wide variety of materials, including meteorite and lunar samples (Wagner et al. 1987), and none of them appear to be good analogs for Lutetia's surface. The feldspar powders have a sharp albedo drop near 3000 Å and have NUV-FUV albedos similar to that of Lutetia, but the ratios between their visible and UV albedos are several times larger than we find for Lutetia.  $\text{SO}_2$  frost also has a sharp drop in albedo near 3000 Å and an FUV albedo in the range of 10–15%, both of which are consistent with Lutetia's UV spectrum. However, the visible-to-UV albedo ratio of  $\text{SO}_2$  frost is several times larger than Lutetia's, and exposed frost isn't expected to be present on Lutetia's surface. The albedos of chondritic meteorite samples are significantly smaller than Lutetia's albedo at all wavelengths, in addition to not matching Lutetia's spectral variations. Similarly, lunar samples tend to have lower UV albedos than Lutetia. Spectra of various mineral powders (e.g., iron, clays, sulfur) also show striking differences when compared to Lutetia's spectrum. Perhaps some mixture of samples could be found to approximate Lutetia's spectrum, but such an effort is beyond the scope of this paper. We note, however, that many of the materials measured by Wagner et al. (1987) have spectral features shortward of 2000 Å, which are potentially observable by the *Alice* instrument during the *Rosetta* flyby.

#### 4. Conclusion

Using the *Hubble Space Telescope*, we measured the albedo of asteroid (21) Lutetia over a wide wavelength range, extending from the far ultraviolet ( $\sim 1500$  Å) to the visible ( $\sim 6000$  Å). The *HST* results reported here suggest a sharp drop in Lutetia's albedo near 3100 Å, and an essentially constant FUV albedo of  $\sim 10\%$  between 1400–3000 Å. The absolute value and spectral variation of Lutetia's UV-visible albedo is not well-matched by the spectra of any meteorites measured in the laboratory. Lutetia may well be composed of material that is either rare or not yet represented in our meteorite collections.

Lutetia's FUV albedo is considerably higher than the values measured for C-chondrites and the Earth's Moon ( $\sim 4\%$ ), which implies that Lutetia should be a relatively easy target for the *Alice* instrument when it makes observations during the *Rosetta* close flyby in July 2010.

*Acknowledgements.* We thank the STScI Director, Matt Mountain, for granting us discretionary observing time for the *HST* Lutetia observations. We thank the STScI ground system personnel, and especially Alison Vick, for successfully planning and executing the observations. We gratefully acknowledge Jennifer Mack and John Biretta for discussions on “red leaks” and for providing the best available *ACS/SBC* and *WFPC2* system throughputs. We thank the other members of the Merline-Drummond ground-based observing team, particularly Al Conrad and Benoît Carry, for providing results on the size and shape of Lutetia prior to publication. The comments of an anonymous reviewer were helpful and have led to several improvements in the paper.

#### References

- A'Hearn, M. F., Feaga, L. M., Steffl, A. J., et al. 2010, *Planet. Space Sci.*, doi: 10.1016/j.pss.2010.03.005
- Baer, J., Milani, A., Chesley, S., & Matson, R. D. 2008, in *Bulletin of the American Astronomical Society*, Vol. 40, *Bulletin of the American Astronomical Society*, 493–+
- Barucci, M. A., Fornasier, S., Dotto, E., et al. 2008, *A&A*, 477, 665
- Barucci, M. A., Fulchignoni, M., Fornasier, S., et al. 2005, *A&A*, 430, 313
- Barucci, M. A., Fulchignoni, M., & Rossi, A. 2007, *Space Science Reviews*, 128, 67
- Belskaya, I. N., Fornasier, S., Krugly, Y. N., et al. 2010, *A&A*
- Bowell, E., Chapman, C. R., Gradie, J. C., Morrison, D., & Zellner, B. 1978, *Icarus*, 35, 313
- Carry, B., Kaasalainen, M., Leyrat, C., et al. 2010, *A&A*, submitted
- Chapman, C. R., Morrison, D., & Zellner, B. 1975, *Icarus*, 25, 104
- Chapman, C. R. & Salisbury, J. W. 1973, *Icarus*, 19, 507
- Clark, B. E., Ockert-Bell, M. E., Cloutis, E. A., et al. 2009, *Icarus*, 202, 119
- Colina, L., Bohlin, R. C., & Castelli, F. 1996, *AJ*, 112, 307
- Drummond, J., Conrad, A., Merline, W., et al. 2010, *A&A*, submitted
- Fienga, A., Laskar, J., Morley, T., et al. 2009, *A&A*, 507, 1675
- Gaffey, M. J. 1976, *J. Geophys. Res.*, 81, 905
- Henry, R. C., Feldman, P. D., Kruk, J. W., Davidsen, A. F., & Durrance, S. T. 1995, *ApJ*, 454, L69+
- Keller, H., Barbieri, C., Koschny, D., et al. 2010, *Science*, in press
- Lazzarin, M., Marchi, S., Moroz, L. V., & Magrin, S. 2009, *A&A*, 498, 307
- Magri, C., Nolan, M. C., Ostro, S. J., & Giorgini, J. D. 2007, *Icarus*, 186, 126
- Magri, C., Ostro, S. J., Rosema, K. D., et al. 1999, *Icarus*, 140, 379
- McCord, T. B. & Chapman, C. R. 1975, *ApJ*, 195, 553
- Merline, W., Drummond, J., Conrad, A., et al. 2010, *A&A*, to be submitted
- Morrison, D. 1977, *Icarus*, 31, 185
- Mueller, M., Harris, A. W., Bus, S. J., et al. 2006, *A&A*, 447, 1153
- Nedelcu, D. A., Birlan, M., Vernazza, P., et al. 2007, *A&A*, 470, 1157
- Perna, D., Dotto, E., Lazzarin, M., et al. 2010, *A&A*, 513, L4+
- Rivkin, A. S., Howell, E. S., Britt, D. T., et al. 1995, *Icarus*, 117, 90
- Rivkin, A. S., Howell, E. S., Lebofsky, L. A., Clark, B. E., & Britt, D. T. 2000, *Icarus*, 145, 351
- Roettger, E. E. & Buratti, B. J. 1994, *Icarus*, 112, 496
- Shepard, M. K., Clark, B. E., Nolan, M. C., et al. 2008, *Icarus*, 195, 184
- Stern, S. A., Slater, D. C., Scherrer, J., et al. 2007, *Space Science Reviews*, 128, 507
- Vernazza, P., Brunetto, R., Binzel, R. P., et al. 2009, *Icarus*, 202, 477
- Vernazza, P., Carry, B., Emery, J., et al. 2010, *Icarus*, 207, 800
- Wagner, J. K., Hapke, B. W., & Wells, E. N. 1987, *Icarus*, 69, 14
- Zellner, B. & Gradie, J. 1976, *AJ*, 81, 262

**Table 1.** Log of *HST* observations of Lutetia.

Visit Info	Measurements	Objectives
ub9h01xxx	WFPC2/PC, 2 dither points	Near-UV albedo
2008-Nov-30	F218W, 4 × 160 s	Bridge from FUV to Visible albedo
17:05-17:45 UT	F255W, 4 × 40 s	
	F300W, 2 × 2 s F606W, 2 × 0.11 s	
ub9h02xxx	ACS/SBC	Far-UV albedo for one hemisphere
2008-Nov-30	F140LP, 1 × 1270 s	
18:40-19:25 UT	F165LP, 1 × 1270 s	
ub9h03xxx	WFPC2/PC, 2 dither points	Visible albedo
2008-Nov-30	F606W, 2 × 0.11 s	Deep probe for dust debris
20:17-20:58 UT	F606W, 3 × 40 s	Deep probe for companions
	F606W, 7 × 160 s	
ub9h04xxx	WFPC2/PC, 2 dither points	Verify putative companions
2008-Nov-30	F606W, 2 × 0.11 s	Repeat of ub9h03xxx
21:52-22:33 UT	F606W, 3 × 40 s	
	F606W, 7 × 160 s	
ub9h05xxx	ACS/SBC	Far-UV albedo for opposite hemisphere
2008-Nov-30	F140LP, 1 × 1270 s	
23:27-00:13 UT	F165LP, 1 × 1270 s	
ub9h13xxx	WFPC2/PC, 2 dither points	<i>B-V</i> color of Lutetia and companions
2008-Dec-15	F606W, 2 × 0.11 s, 2 × 40 s, 2 × 160 s	
13:26-14:08 UT	F450W, 2 × 0.35 s, 4 × 140 s	
ub9h14xxx	WFPC2/PC, 2 dither points	Verify colors
2008-Dec-16	F606W, 2 × 0.11 s, 2 × 40 s, 2 × 160 s	
13:26-14:06 UT	F450W, 2 × 0.35 s, 4 × 140 s	

**Table 2.** *HST* photometry of Lutetia.

Filter	Measured Signal ( $e\ s^{-1}$ )		Model Signal (Total $e\ s^{-1}$ )
	Total	Error	
F140LP	12.52	0.10	12.52
F165LP	11.69	0.10	11.64
F140LP-F165LP	0.828	0.141	0.879
F218W	33.7	1.7	33.4
F255W	226	7.0	226
F300W	9625	150	9499
F450W	120,160	2400	122,990
F606W	$1.107 \times 10^6$	$4.42 \times 10^3$	$1.122 \times 10^6$



**Fig. 1.** *HST*/*WFPC2* images of asteroid 21 Lutetia taken through the F218W, F255W, F300W, and F450W filters (see identifying labels on the images). Each image is a  $128 \times 128$  pixel subsection (each image is  $5''.89$  across) of the full image and is displayed using an asinh intensity stretch (similar to logarithmic) ranging from approximately zero to the maximum intensity in each image. All images have been rotated so that celestial north points up and east is to the left. The scale bar is  $1''$  across, which subtends 1088 km at Lutetia on December 15 (when the F450W image was taken), and 1044 km on November 30 (when all the other images were taken). Each image is a composite of at least two separate images taken with Lutetia centered at two different locations on the CCD. The “tails” apparent on two of the images are low-level artifacts caused by degraded charge transfer efficiency in the *WFPC2* CCD.

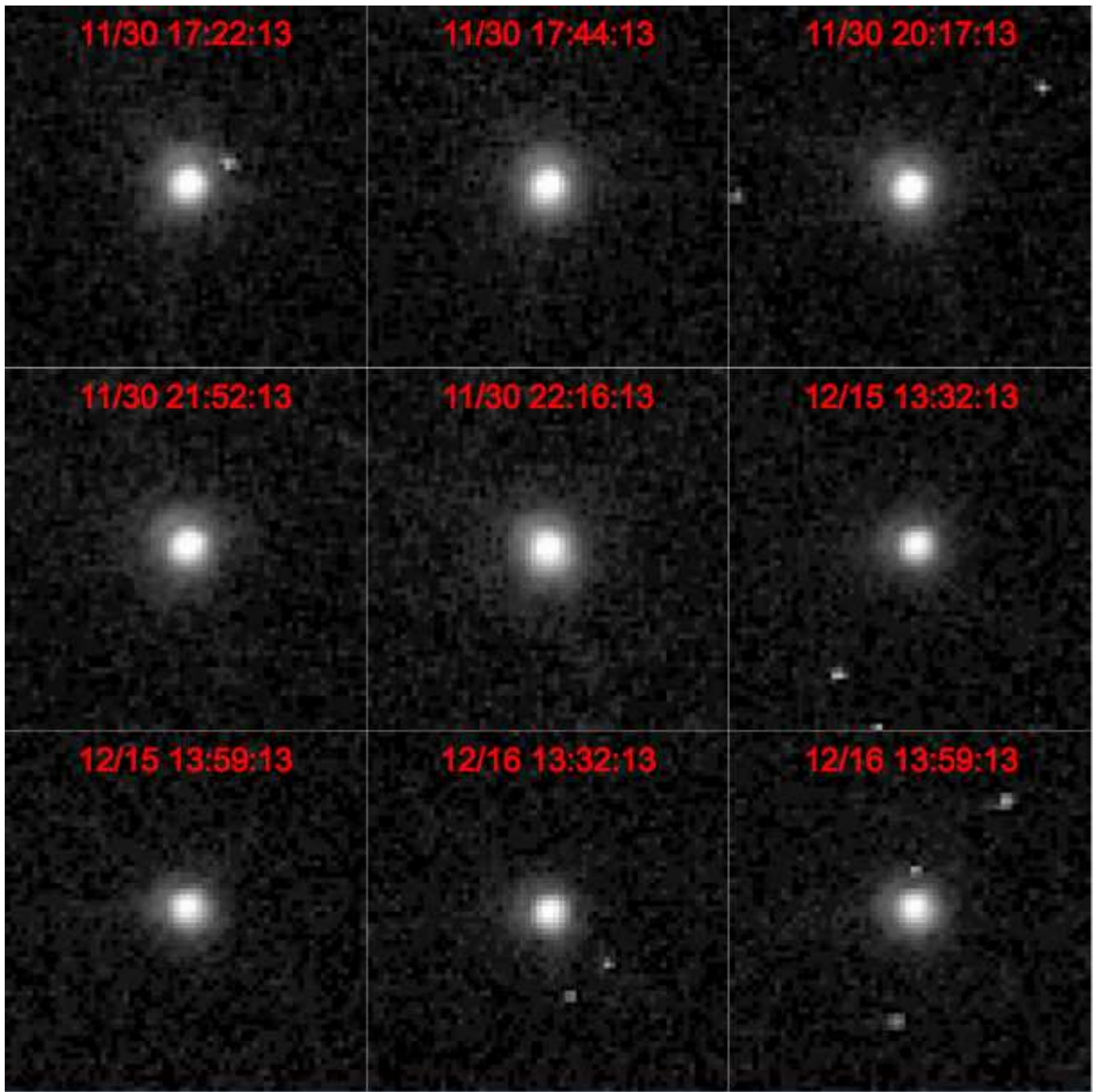


**Fig. 2.** *HST/WFPC2* images of Lutetia taken through the F606W filter with an exposure time of 0.11 s and rotated so that celestial north points up and east is to the left. Each image is a  $64 \times 64$  pixel subsection (each image is  $2''.94$  across) of the full image and is displayed using an asinh intensity stretch (similar to logarithmic) ranging from approximately zero to the maximum intensity in each image. Cosmic ray events are evident in some of the images as clusters of bright pixels. The image start times (UT) are displayed in each frame.



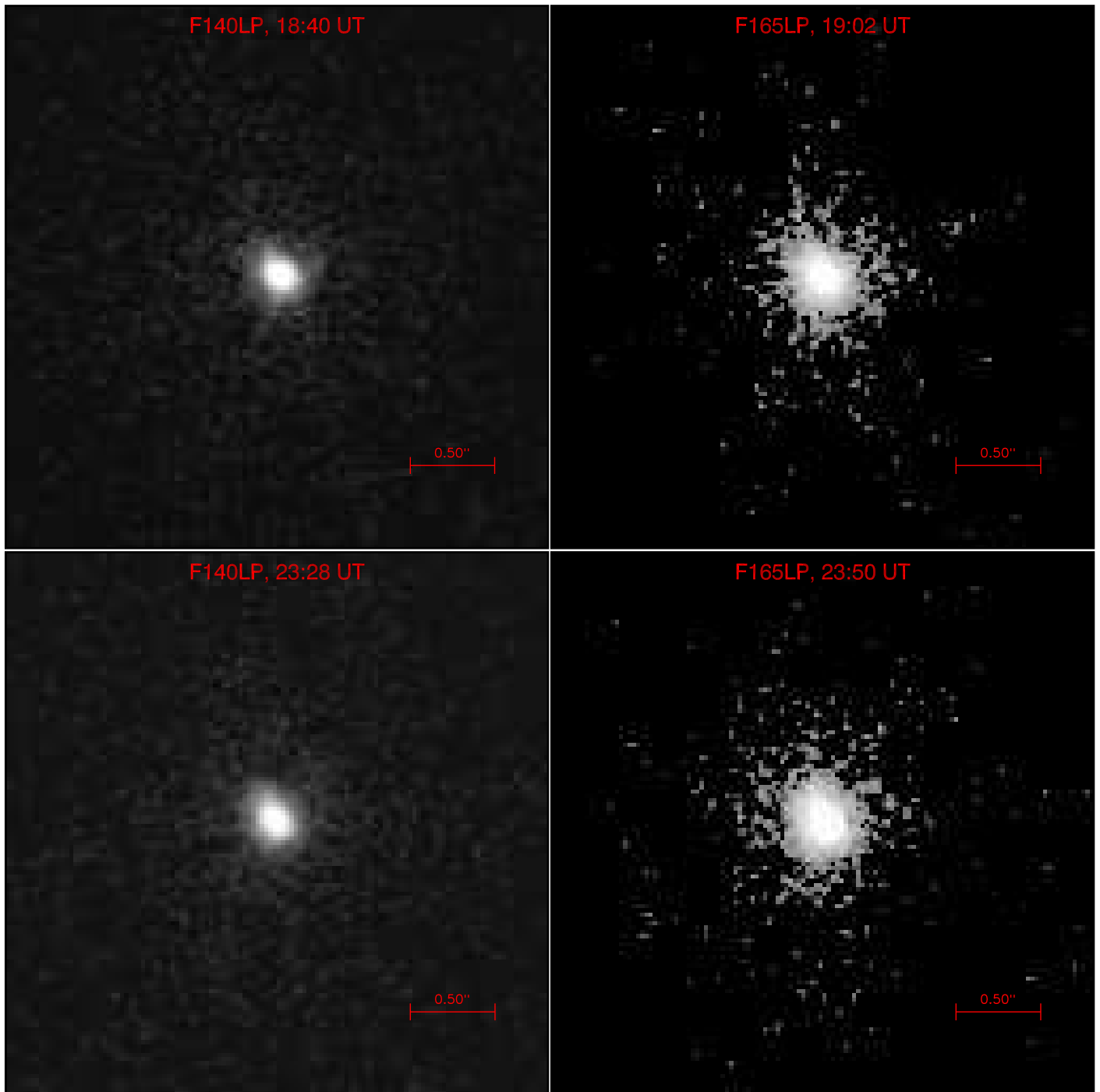


**Fig. 3.** *HST/ACS* images of asteroid 21 Lutetia taken through the F140LP and F165LP filters (see identifying labels). Each image is displayed using an asinh intensity stretch (similar to logarithmic) ranging approximately from zero to the maximum intensity in each image. All images have been rotated so that celestial north points up and east is to the left. The scale bar is  $0'.5$  across, which subtends  $\sim 520$  km on 30 November 2009 when the images were taken (start times are labeled on each image).

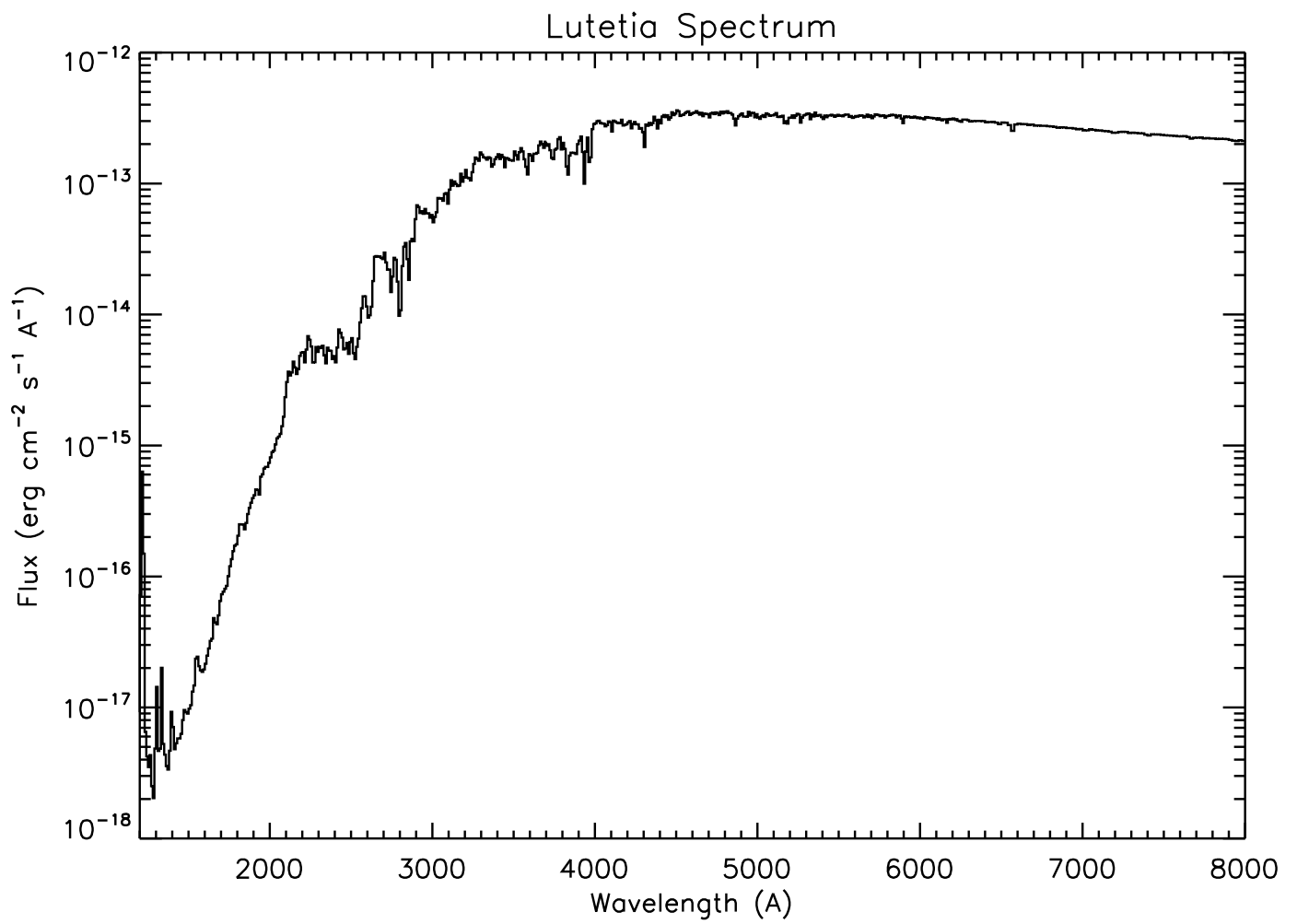


**Fig. 4.** Our best estimate for the Lutetia spectrum at the time of the *HST* observations on 30 November 2008.

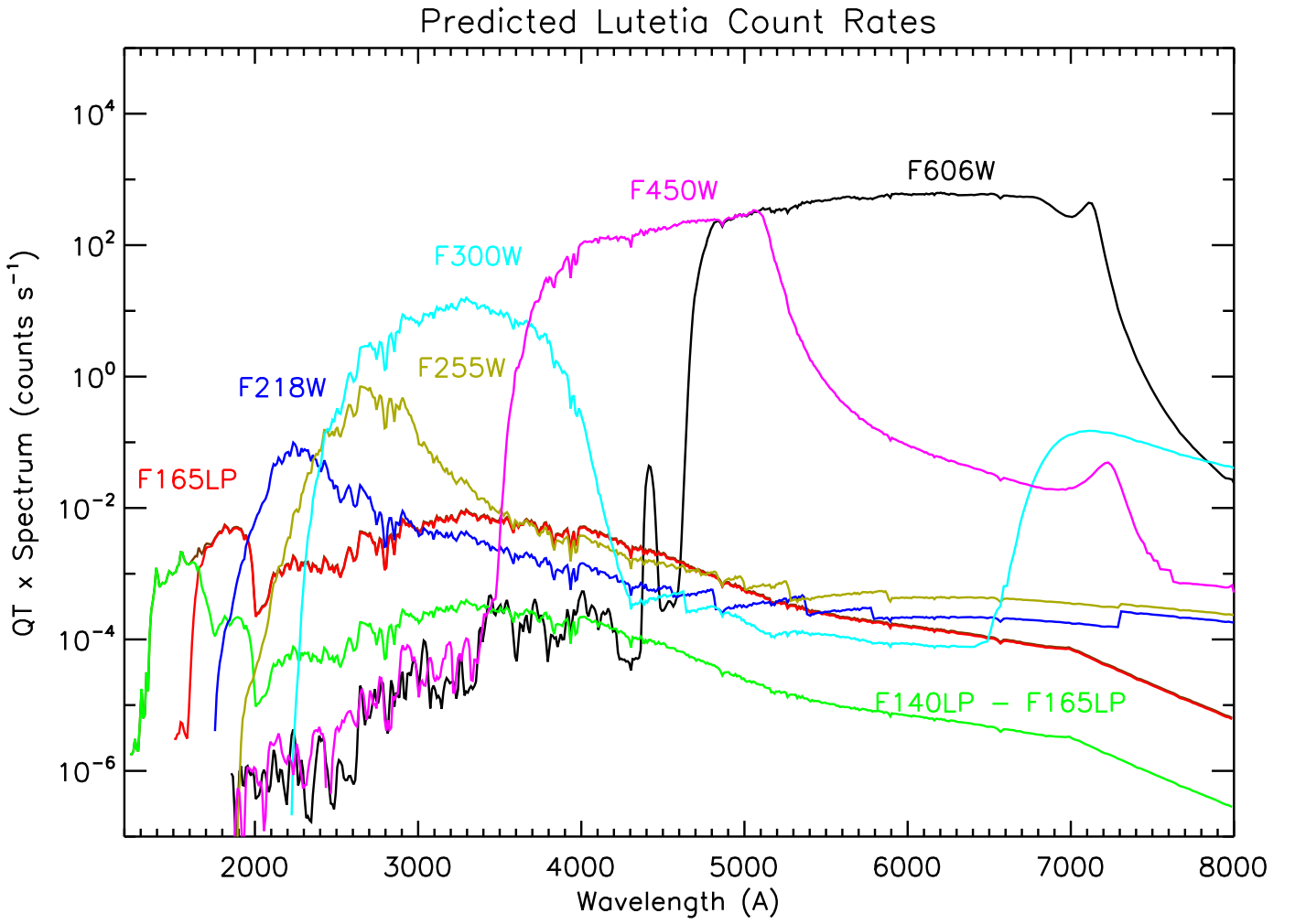


**Fig. 5.** After adopting our best estimate for Lutetia’s flux, we plot the *predicted* count rates as a function of wavelength for each of the filters employed during the *HST* observations. “F140LP–F165LP” refers to the *difference* between the F140LP and F165LP filters. For clarity, the F140LP curve is not explicitly labeled, but it is essentially identical to the F165LP curve longward of 1650 Å and essentially identical to the F140LP–F165LP curve shortward of that wavelength. Note the logarithmic scale.

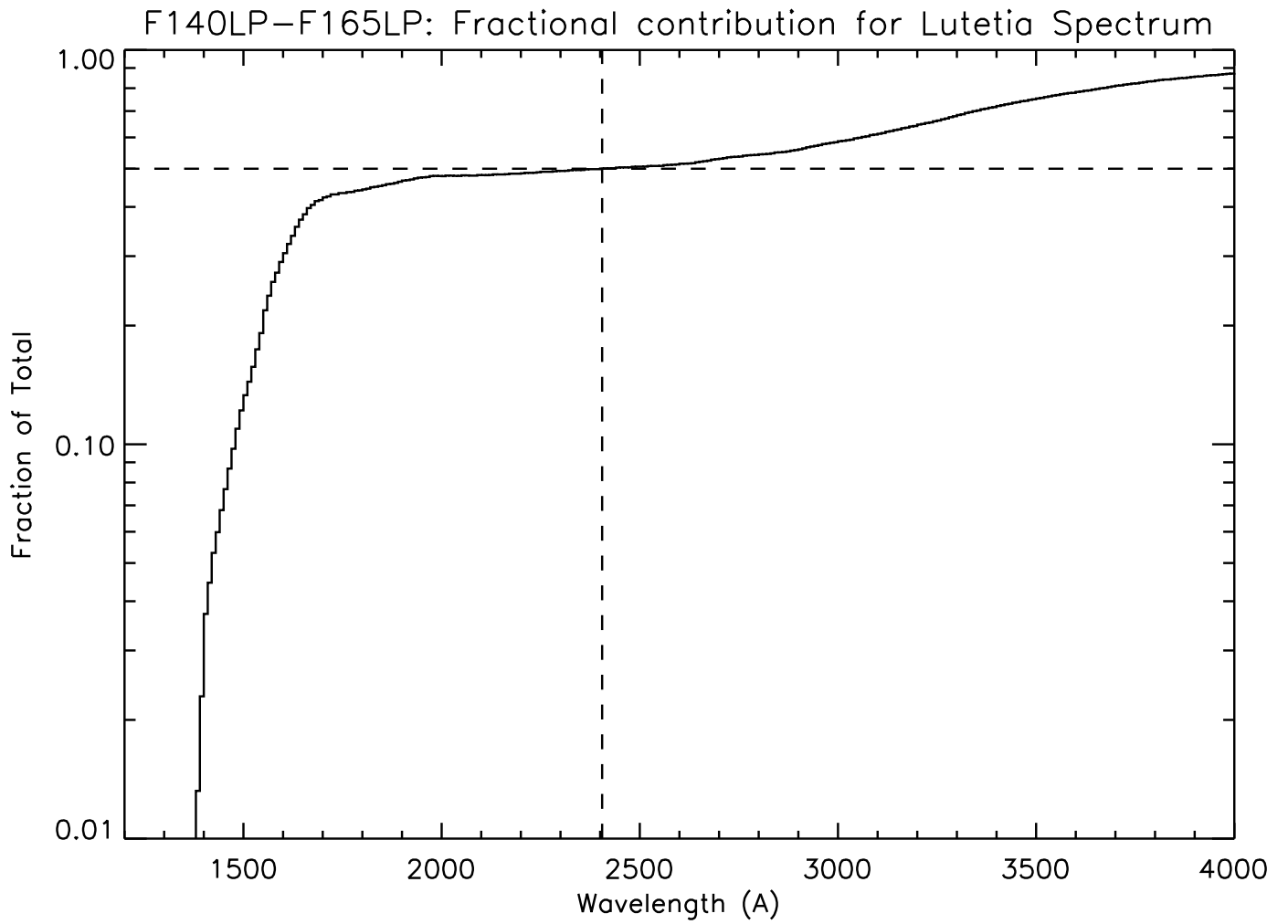


**Fig. 6.** The cumulative fractional contribution to the observed count rate as a function of wavelength for the *difference* (F140LP–F165LP) of the two far-UV filters employed during the *HST* observations. Approximately 40% of the observed signal is produced by photons having wavelengths smaller than 1675 Å, but 50% of the signal is coming from light longward of 2400 Å.



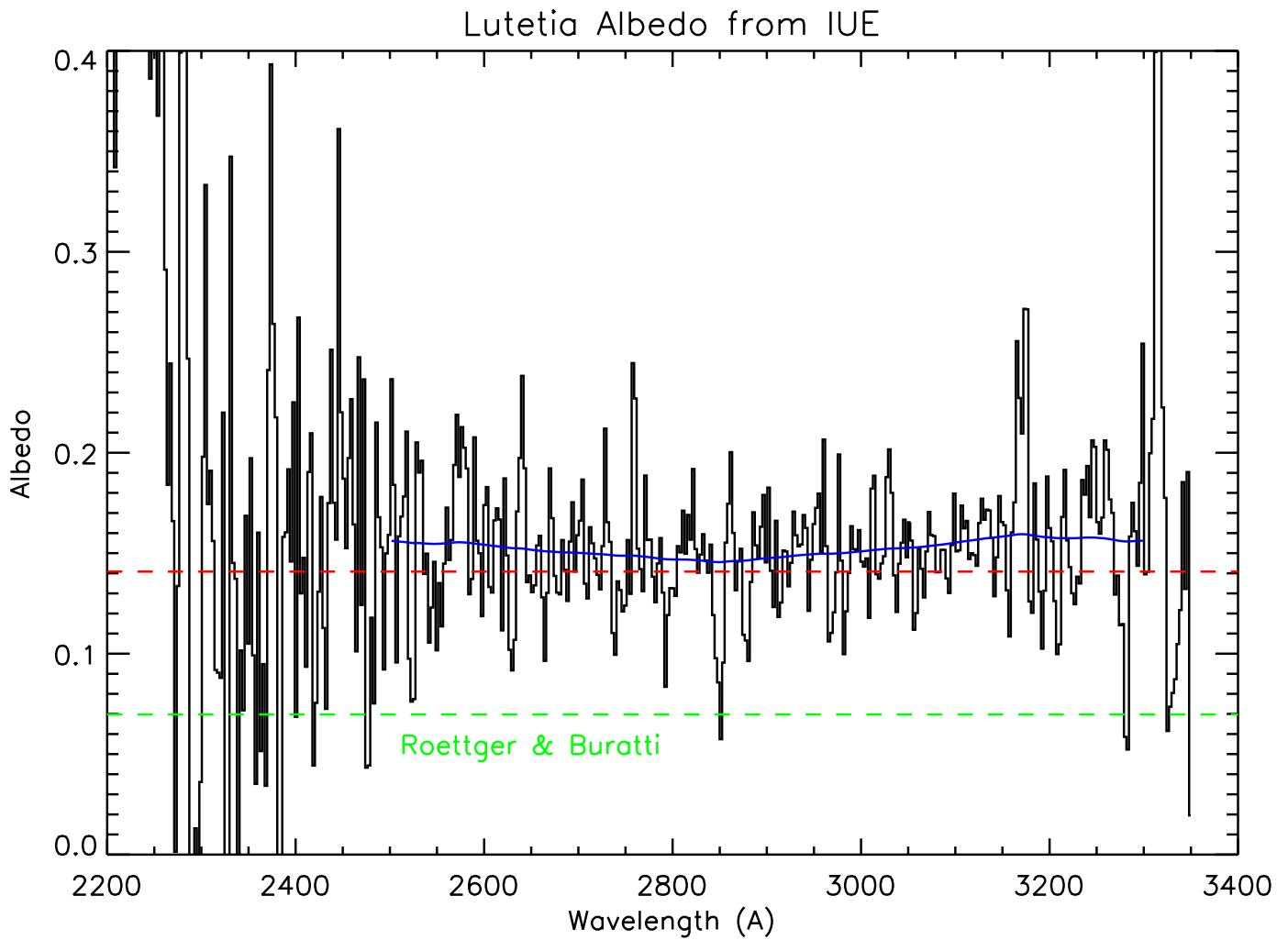


**Fig. 7.** Albedo spectrum of Lutetia derived from *IUE* observations made on 7 January 1982 at a solar phase angle of  $26^\circ.1$ . The albedo at  $2670 \text{ \AA}$  adopted by Roettger & Buratti (1994) is shown by the dashed green line, while our equivalent value, using a different phase correction, is depicted by the dashed red line. The blue curve is a Fourier-filtered version of the *IUE* spectrum, passing only the lowest 1% of spatial frequencies.

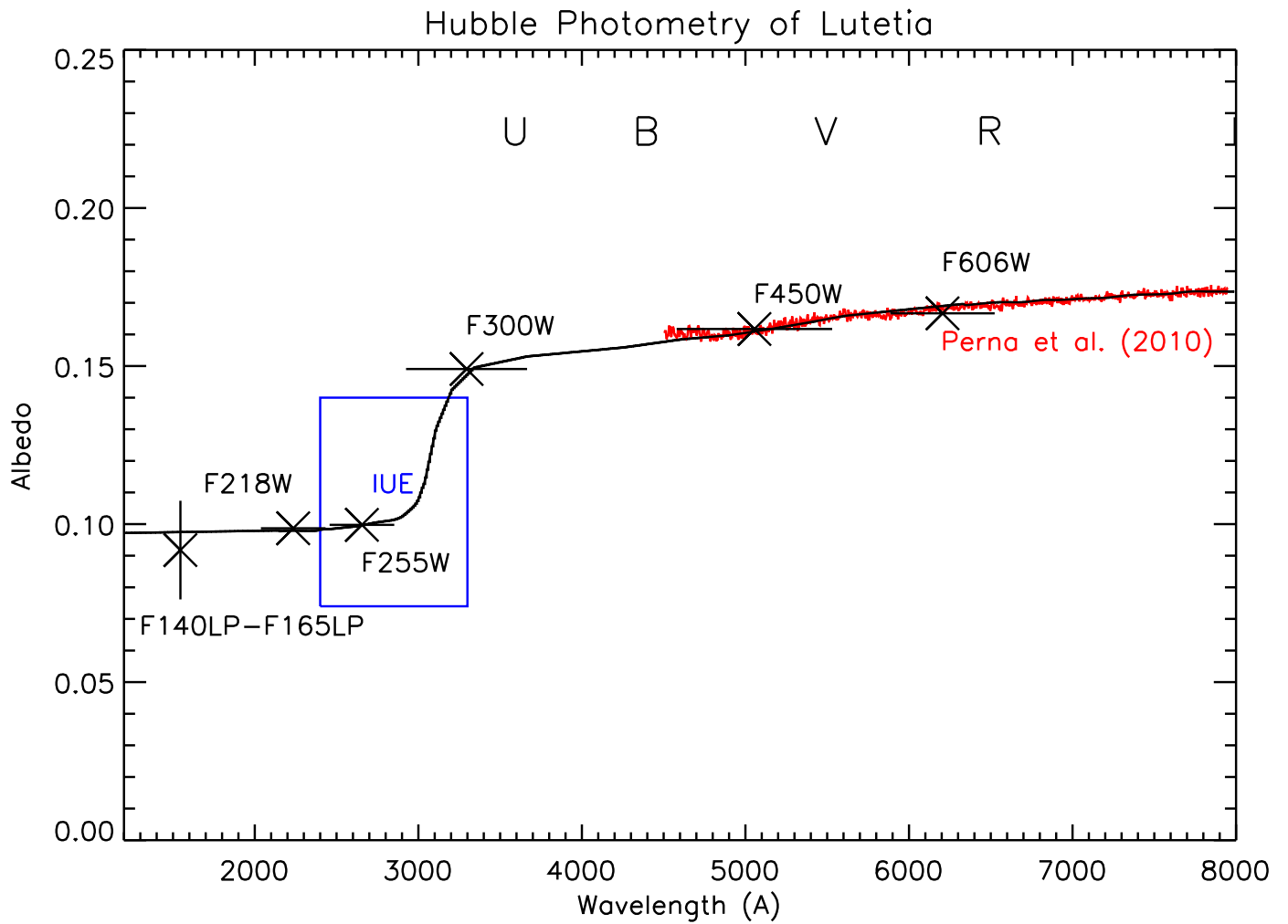


**Fig. 8.** Our best estimate for the albedo of Lutetia is plotted as a solid black line. The spectrum plotted in red is from a ground-based observation taken on 28 November 2008. The blue rectangle shows the wavelength coverage and the range of possible albedos derived from an *IUE* spectrum taken on 7 January 1982. The *HST* data (×) are plotted at the wavelengths where the predicted count rate is largest; the horizontal bars give the “effective bandwidth” of the filters, as specified in the STScI Instrument Handbooks. The wavelengths of the standard *UBVR* bands are also displayed for reference. Only the error bar for the F140LP–F165LP *difference* filter case is displayed because the error bars for the other filters are smaller than the plotting symbols.